RSC Advances

PAPER

View Article Online
View Journal | View Issue

Cite this: *RSC Adv.*, 2021, **11**, 26629

Self- and dis-assembly behavior of segmented wormlike nanostructures from an ABC triblock copolymer†

Kaiyuan Liang,[a] Guohao He,[a] Qimeng Wang,[a] Zhiying Xie,[a] Mingming Li,[b] Xin Li,[b] Haizhou Yu [b] and Xiaoyan Qiu *[a]

Received 13th June 2021
Accepted 27th July 2021

DOI: 10.1039/d1ra04580f

rsc.li/rsc-advances

Herein, we described the self-assembly of a triblock copolymer, poly(styrene-*b*-2-vinylpyridine-*b*-ethylene oxide) (PS-*b*-P2VP-*b*-PEO), in THF/water at room temperature to form segmented wormlike nanostructures. We found two different formation mechanisms of the segmented wormlike nanostructures from PS-*b*-P2VP-*b*-PEO with different molecular weights. Moreover, the dimension of such segmented wormlike nanostructures depends on the stirring rate. Interestingly, these wormlike nanostructures disassembled gradually when increasing the temperature, which is reversible. After cooling to room temperature the segmented wormlike micelles reformed gradually with stirring. Furthermore, neither intense stirring nor ultrasonic vibration could damage the structure of these wormlike nanostructures which proves their stability and potential application as drug delivery vehicles.

Introduction

The spontaneous self-assembly of amphiphilic molecules into discrete supramolecular assemblies and two- and three-dimensional macrolattices has been used in the development of many applications, including nanotechnology and biomedicine.[1–3] The micelles can segregate into distinct nanodomains due to the effective repulsion between the immiscible hydrophobic and hydrophilic blocks of the copolymer.[4–6] Block copolymers, which consist of macromolecules formed by covalent end-linking of two or more disparate polymeric blocks, represent a particularly appealing template material. They offer a host of control variables through which structure may be tuned by molecular parameters including molecular weight and block copolymer composition, and solution parameters like copolymer concentration, solvent compositions, temperature, and others.[7–10] It has been recognized that triblock copolymers can provide an important role in making the phase diagrams more complicated compared with diblock copolymers.[11,12] The main motivation for studying ABC triblock terpolymer micelles is related to the presence of a third nanosized compartment in the micellar structure.[13–15] When dissolved in a solvent selective for one constituent core-shell-corona micelles could be prepared from ABC triblock copolymers.[16]

The multicompartment micellar structures have promising potential applications due to their biological similarity with eukaryotic cells and as nanocontainers to solubilize two or more incompatible agents within separate nanoscopic compartments in a precise stoichiometric ratio.[17–20] Some progress toward multicompartment micelles has been reported; in examples combining three mutually immiscible polymeric components in mixed arm star block terpolymer architecture, Li and coworkers have observed the multicompartment micelles in dilute aqueous solution.[4] Recently, Zhu J. T. and coworkers have successfully synthesized a new type of self-assembled object-giant segmented wormlike nanostructures from a PS-*b*-P2VP-*b*-PEO triblock copolymer. They found that the triblock copolymer aggregated to form spherical micelles *via* primary self-assembly, and then further self-assembled into the giant segmented wormlike nanostructures.[21] In addition, temperature has been used as a tool to control the block copolymer self-assembly for several years.[22–24] The nature of the polymer–solvent interaction is important in these studies. This temperature-dependent micellization and demicellization is specifically useful for temperature-driven drug delivery. For example, reversible morphological changes of PS_{962}-*b*-PEO_{227} induced solely by changing the temperature for fixed copolymer concentration and solvent composition in a DMF/water system have been reported. The changes are reversible and require only a few hours of equilibrating for the forward and backward changes.[25]

Block copolymers having a poly(ethylene oxide) (PEO) water-soluble block comprise a special and interesting category since

[a]*Key Laboratory of Flexible Electronics (KLOFE), Institute of Advanced Materials (IAM), Nanjing Tech University, Nanjing 211816, Jiangsu Province, PR China. E-mail: iamxyqiu@njtech.edu.cn*

[b]*Institute of Advanced Synthesis (IAS), School of Chemistry and Molecular Engineering, Nanjing Tech University, Nanjing 211816, Jiangsu Province, PR China*

† Electronic supplementary information (ESI) available. See DOI: 10.1039/d1ra04580f

PEO is a crystalline, neutral, and biocompatible material.[26,27] In addition, the triblock copolymer PS-*b*-P2VP-*b*-PEO might exhibit more fantastic structure and property diversity than we thought. In this paper, we present another type of segmented wormlike nanostructure from PS-*b*-P2VP-*b*-PEO. The direction of orientation of the segmented parts, *i.e.*, disks, is found perpendicular or parallel to the main axis. We found two formation mechanisms of this kind of wormlike nanostructures from two triblock copolymer with different molecular weights. And the dimension of the nanostructures was found to be dependent on the stirring rate. Furthermore, the reversible morphological transition of these wormlike nanostructures induced by increasing the temperature is investigated. We found that the wormlike nanostructures were formed *via* the self-assembly of the triblock copolymer at room temperature (20 °C) in THF/water solution, and disassemble gradually upon increasing the temperature. Moreover, the disassembled nanostructures after cooling to room temperature will self-assembly again to form the segmented wormlike nanostructures under stirring.

Experimental section

Materials

Four poly(styrene-*b*-2-vinylpyridine-*b*-ethylene oxide) (PS-*b*-P2VP-*b*-PEO) triblock copolymers with different compositions (the subscript numbers represent the number of repeat units of the blocks), *i.e.*, PS_{720}-*b*-$P2VP_{200}$-*b*-PEO_{363} (M_n = 112 000 g mol^{-1}), PS_{768}–$P2VP_{133}$–PEO_{95} (M_n = 98 000 g mol^{-1}), PS_{720}-*b*-$P2VP_{200}$-*b*-PEO_{375} (M_n = 112 500 g mol^{-1}), PS_{432}-*b*-$P2VP_{152}$-*b*-PEO_{193} (M_n = 69 500 g mol^{-1}), were purchased from Polymer Source Inc. Canada. Hydrochloric acid (HCl) was purchased from Aladdin. Tetrahydrofuran (THF) was obtained from Sigma-Aldrich.

Preparation of nanostructures

To prepare the nanostructures, copolymer was firstly dissolved in tetrahydrofuran (THF), which is a solvent for all of three types of the blocks. The initial block copolymer concentration was 1.0 wt%. The copolymer solution was kept stirring overnight to make sure that the solution was homogenous. Then, deionized water was added to the solution at the approximate rate of 0.2 wt%/30 s with proper stirring to induce the self-assembly of the block copolymer. A total of *ca.* 13 wt% water was added to the block copolymer solution. This solution, at this water content, was kept stirring for one day. Subsequently, a large amount of distilled water (*ca.* 400 wt%) was added to the resulting solution to quench the micellar morphologies. The final solution was placed in dialysis bags and dialyzed against distilled water for one day to remove all of the organic solvent from the solution.

For studying the effect of temperature, the solutions in vials were sealed with Teflon tape and kept at the desired temperature in a temperature-controlled oil bath with a digital temperature controller having an accuracy of ±0.1 °C. In order to study the morphological evolution in an isothermal condition where the morphological changes occur, the samples were taken out of the isothermal temperature oil bath at different temperatures and then quenched by adding them to excess of water for TEM sample preparation.

Field emission scanning electron microscopy (SEM)

Scanning electron microscope (SEM) (QUANTA FEG 250) was used to observe morphology of the nanostructures with an accelerating voltage of 10 kV. Field emission scanning electron microscope (FESEM) images were obtained using an FEI Quanta 600 series microscope at 10 kV with a working distance of 10 mm. One drop of the dilute solution was dropped onto the silicon (Si) wafers and dried then placed on a specimen holder using carbon conductive tapes. To avoid charging problems, the samples were sputter coated with gold for 60 s at 20 mA current in a vacuum atmosphere.

Transmission electron microscopy (TEM) and staining experiment

Transmission electron microscopy (TEM) images were obtained by using a TALOS L120C transmission electron microscope (TALOS, Czech Republic) with an acceleration voltage of 100 kV. Since we need to visualize the morphology in the solution at the particular temperature, a small amount of the solution was quenched in excess water at room temperature. A drop from the quenched solution was then placed on the carbon-coated grid. After a few minutes, the excess solution was blotted with filter paper. The grids were dried at room temperature and atmospheric pressure for several hours before observation using the TEM.

The PS blocks were in their glassy state, therefore, the "quenched" morphologies were fixed during TEM observation. Designated samples were stained by phosphotungstic acid ($H_3PO_4 \cdot 12WO_4$) aqueous solution onto the surface of the sample-loaded grid. Three minutes later excess solution was blotted with a filter paper. The samples was then gently washed with water and dried in air at room temperature before TEM observation.

Atomic force microscopy (AFM)

The resulting morphologies were visualized with SPA-300HV atomic force microscopy. To prepare the samples for AFM, a drop of the resulting solution was placed on the silicon wafers. Prior to coating, the silicon substrates were cleaned in a bath of 100 ml of 80% H_2SO_4, 35 ml of H_2O_2, and then carefully rinsed with deionized water. The silicon surface was then dried with compressed nitrogen gas. The coated substrates were then dried in air and at room temperature for one day before observation.

Turbidity measurements

All turbidity measurements were performed on a Shimadzu UV-2450 ultraviolet-visible (UV-vis) spectrometer. The instrument was set at the absorbance (turbidity) mode, and measurements were recorded every 0.02 min at λ = 650 nm. At this wavelength the copolymer has minimal absorption, and any attenuation of

light is due to scattering from the micellar aggregates. THF was used as the referee for all the measurements.

Dynamic light scattering

DLS measurements were performed with a Malvern NanoZS Zetasizer equipped with a 633 nm He–Ne laser. The *x* potential of the samples was obtained with Zetaplus. All DLS measurements were done with a laser wavelength of 658.0 nm and an incident angle of 90° at 25 °C. For each sample, 15 runs of 10 s were performed, with three repetitions.

Results

Fig. 1 displays the typical TEM micrograph of PS_{720}-*b*-$P2VP_{200}$-*b*-PEO_{363} (the subscript numbers represent the number of repeat units of the blocks) triblock copolymer that exhibits the segmented wormlike nanostructures. Besides the wormlike structures, only spherical micelles were observed in this system (Fig. 1a and b). These nanostructures are layered or segmented along their axis, looking like shuttle (fusiform profile. *i.e.* the diameters were larger in the middle). This might be resulted from the shear field since intense stirring (1000 rpm) is performed to drive the self-assembly of the triblock copolymers. The segmented wormlike nanostructures are gigantic with the length of several micrometers. From the TEM images we can observe that these wormlike structures are composed of the same elemental units (Fig. 1 and S1†), *i.e.*, the disks, which are more or less similar with the objects found by Zhu J. T.[21] But there are still several significant differences. One is that the disks in present work having different diameters (*ca.* 125–400 nm), but approximately identical thickness (*ca.* 67 nm), are ranked closer to each other (Fig. 1b) compared with previous work. This might be attributed to the difference of the composition of the triblock copolymer. The segmented wormlike nanostructures are so sensitive to the block length of the copolymer in present work, which means only the triblock copolymer with proper compositions can self-assemble to form such giant segmented wormlike nanostructures. Fig. S2† displays the AFM images of assembled spherical micelles prepared from PS_{432}-*b*-$P2VP_{152}$-*b*-PEO_{193} (Fig. S2a†), and giant micelles prepared from PS_{720}-*b*-$P2VP_{200}$-*b*-PEO_{375} (Fig. S2b†) in THF/water solutions. Obviously, these copolymers are hard to form segmented wormlike nanostructures even with a little longer hydrophiphilic PEO blocks (Fig. S2b†) compared with PS_{720}-*b*-$P2VP_{200}$-*b*-PEO_{363} (Fig. 1). So far, the boundary of the segmented wormlike nanostructures formation is being explored, since triblock copolymer is a kind of complex system. We deduce that the repulsive interaction among the corona blocks plays a critical role since it changes with the length of the corona blocks as has been reported in previous work.[28]

Another interesting difference of present wormlike structures is that the direction of orientation of the segmented parts, *i.e.*, disks, is found either perpendicular or parallel to the main axis (Fig. 2a). After selectively stained by $H_3PO_4 \cdot 12WO_4$ (P2VP domains appear dark at the periphery of the disks) one can clearly see the orientation of the disks in Fig. 2a. Furthermore, you can observe the disks both perpendicular and parallel to the main axis in one "worm" (Fig. 2b–d). Details regarding why disks like to stack together along different direction are currently under investigation. However, the slow kinetics of block copolymers in solution, due to the slow exchange of chains between micelles because of the higher molecular weight of the molecules, hinders assembled structures from reaching global equilibrium states. In addition, the flow filed in the solution is not uniform. The flow rate in some local regions is relatively high.[29] Therefore, many fantastic intermediate states could be occasionally captured, like earthworm (Fig. 3a), necklace (Fig. 3b), seahorse (Fig. 3c), finger print (Fig. 3d) and giant worms (Fig. 3e) in our studies.

To reveal the mechanism of the formation of the segmented wormlike nanostructures, samples from different block copolymer were extracted from the solution mixture at different stirring times at room temperature (20 °C). We kept the stirring rate constant, *i.e.*, 1000 rpm. The intermediate structures can then be trapped by quickly adding the extracted solutions to an excess of water, and then studied by using SEM. It is should be noted that a large number of such nanostructures were obtained in experiments. Only individual one was recorded and given here in order to exhibit the microstructure clearly. Fig. 4a–d displays the structures at different stages of the wormlike structures formation from PS_{720}-*b*-$P2VP_{200}$-*b*-PEO_{363}.

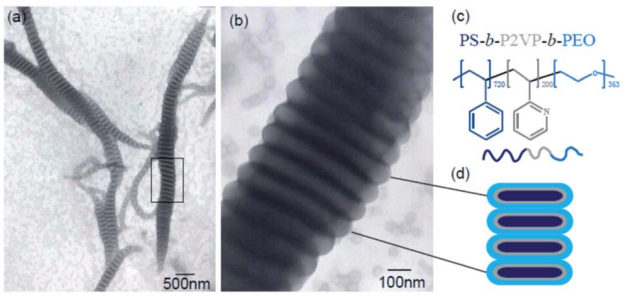

Fig. 1 (a) TEM image of the segmented wormlike nanostructures formed from PS_{720}-*b*-$P2VP_{200}$-*b*-PEO_{363} at room temperature (20 °C); (b) is the enlarged image of the squared place in Fig. 4a; (c) molecular structures of triblock copolymer, PS_{720}-*b*-$P2VP_{200}$-*b*-PEO_{363}; (d) schematic drawing of cross section of the segmented parts.

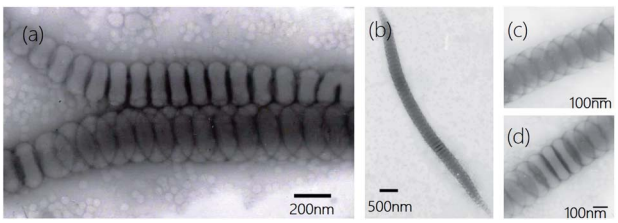

Fig. 2 (a) Two segmented wormlike nanostructures from PS_{720}-*b*-$P2VP_{200}$-*b*-PEO_{363} with the disks parallel or perpendicular to the main axis; (b) single segmented wormlike nanostructure with the disks parallel and perpendicular to the main axis; (c) and (d) are the enlarged images of the local places in (b).

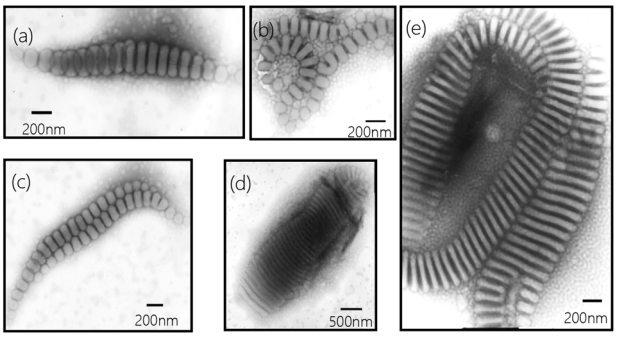

Fig. 3 Representative TEM images (a–e) of intermediate structures trapped from 1 wt% of PS_{720}-*b*-$P2VP_{200}$-*b*-PEO_{363} in THF/water (water content 15 wt%) after stirred for four days.

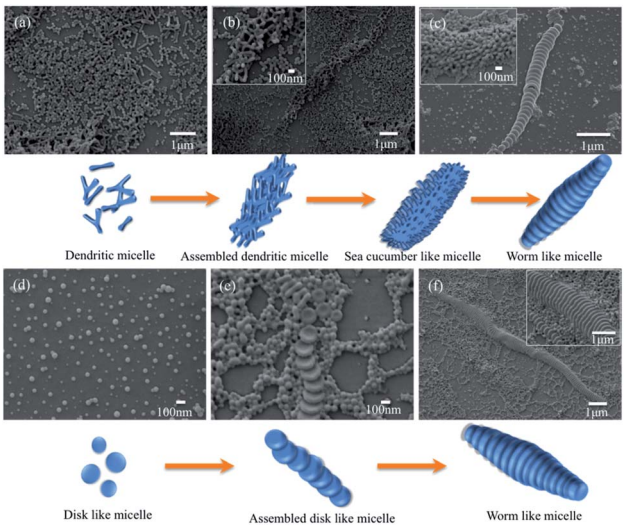

Fig. 4 SEM images show two formations mechanisms of the segmented wormlike nanostructures from PS_{720}-*b*-$P2VP_{200}$-*b*-PEO_{363} annealing for (a) 24 h; (b) 48 h; (c) 96 h; and from PS_{768}–$P2VP_{133}$–PEO_{95} annealing for (d) 20 h; (e) 50 h; (f) 96 h at room temperature (20 °C), in THF/H_2O mixtures (water content: 13 wt%).

We found that the formation of segmented wormlike nanostructure from PS_{720}-*b*-$P2VP_{200}$-*b*-PEO_{363} underwent four stages. The initial morphology was a mixture of small spheres and dendritic micelles (Fig. 4a), and then as time went on, these dendritic micelles tend to assemble to form the assembled structures (Fig. 4b). Then, more and more dendritic micelles assembled to form the sea cucumber like structures with stirring (inset image in Fig. 4c). Finally, these structures rearranged and self-assembled to form the segmented wormlike nanostructures (Fig. 4c). When the triblock copolymer was replaced with the PS_{768}–$P2VP_{133}$–PEO_{95}, the formation process and morphology of wormlike structures had a great change. Dominant morphology was spherical micelle at first, and with the increase of the stirring time, disk like structures gradually appeared (Fig. 4d). It is worth noting that in the whole process no other shapes, such as rod-like or ring-like shapes in Fig. 4, have been observed except spherical micelles and disk like structures. From this we can infer that the wormlike nanostructures are stacked by disk like structures, which begins with small spheres, and then the disks aggregate and fuse with the surrounding micelles into assembled disc like structures (Fig. 4e). With stirring, the disk like structures and surrounding micelles overlapped in an orderly manner to form wormlike nanostructures eventually (Fig. 4f). The responding dynamic light scattering (DLS) results exhibit the dimension evolution of the segmented wormlike nanostructures (Fig. S3†). We found that the trends of DLS results match well with the SEM images.

These worm-like nanostructures were segmented in the direction of the long axis, and the overall profile was in the form of a shuttle or a streamline shape. The middle part of the disk had the largest diameter, about 400 to 1000 nm. The closer to both ends, the smaller the diameter of the plate and the end of the disk was in the shape of small ball. Studies have shown that spherical micelles can be joined together by nonspecific-force.[30] The molecular structure of the triblock copolymer is shown in Fig. 1c. When the spherical micelles approach to each other, any fluctuations in the PEO and P2VP microdomains will expose the hydrophobic PS core. Due to the presence of shear flow, the micelles move continuously in the direction of the flow field in the container. When the spherical micelles gradually assemble, they tend to form a streamlined or shuttle-like structure to reduce the resistance of the micelles during the movement. During the assembly process, water molecules and hydrophilic blocks will constantly out of the aggregates (shuttle-like structures), and the same components will fuse to form a common microdomain. Under the shear condition, THF fully swells the PS block, allowing the mergence of the spheres to smoothly transition to the segmented wormlike nanostructures. The flow field under shearing tends to concentrate the spheres along the main axis of the shuttle-like structure, while the fusion and adjustment of the spheres is perpendicular to the major axis of the shuttle-like structure, so that the plane of the disks is formed in a direction perpendicular to the main axis. With the increase of the annealing time, the intermediate structure decreases and the segmented wormlike structures become more.

In addition, we are surprised to find that the dimensions of the nanostructures are also affected by the stirring rate. To a certain extent, the higher the shear rate, the longer the length of the nanostructures formed. When the speed reaches 1500 rpm, the maximum length can reach several tens of

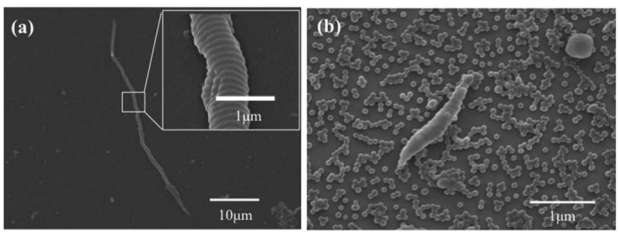

Fig. 5 Morphology formed from PS_{720}-*b*-$P2VP_{200}$-*b*-PEO_{363} copolymer at (a) 1500 rpm stirring rate, inset is the enlarged image of the squared place; (b) 200 rpm stirring rate.

microns (Fig. 5a). This might be resulted from the intense shear field. The long structures decrease the degree of the stretching of the core chains, which is not favorable for the formation of the segmented wormlike nanostructures. However, when the rate is high and the force given by the shear field is strong enough, the wormlike nanostructures can be maintained for a long length, even if the repulsive interaction between the corona blocks raises. The shear force increases the degree of the stretching of the core chains, which is favorable for the formation of the segmented wormlike nanostructures. When the stirring rate is deceased to 200 rpm, only short wormlike structures could be found occasionally with dominant spherical micelles. We believe that intense shear field is advantageous to the assembly of the spherical or disk like structures. In present work, stirring rate beyond 800 rpm is better for the formation of segmented wormlike nanostructures.

These nanostructures are temperature sensitive. These wormlike nanostructures disassembled gradually to the initial state upon increasing the temperature from 20 °C to 30 °C, 40 °C, 50 °C and 55 °C (Fig. 6e–a). More intermediate structures during heating were exhibited in Fig. S4.† We can clearly see the damage of the disks upon heating and the disks disassemble to packed spheres (Fig. 6b and S4†). The possible mechanism for the inverse change of the wormlike nanostructures might be the mixture (THF/water) is a poor media for PS blocks, while a nice solvent for the hydrophiphilic P2VP and PEO blocks. When increasing the temperature solvent (water) quality becomes worse for the P2VP and PEO blocks due to the destruction of hydrogen bonds existing between the hydrophiphilic chains and water molecules.[31,32]

On the other hand, as the temperature increases the mixed solvent becomes less poor for PS blocks. This can be supported from the critical water concentration (CWC) experiment in Fig. 7. Water is a poor solvent for PS blocks, and more and more PS chains aggregate with the addition of water. At the beginning of the water addition, the turbidity intensity is almost constant. When the water concentration exceeds a critical value, the turbidity (absorbance) has a break jump indicating the micellization has taken place (Fig. 7c). An approximate value of the critical water concentration is thus obtained from the intercept

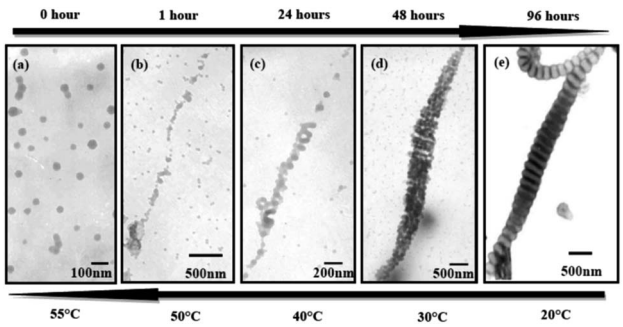

Fig. 6 Morphological changes from the self-assembly (a–e) of a system with 1.0 wt% copolymer and 15 wt% water concentration in THF/water after stirred for 4 days; and disassembly (e–a) upon heating the same system in 30 min.

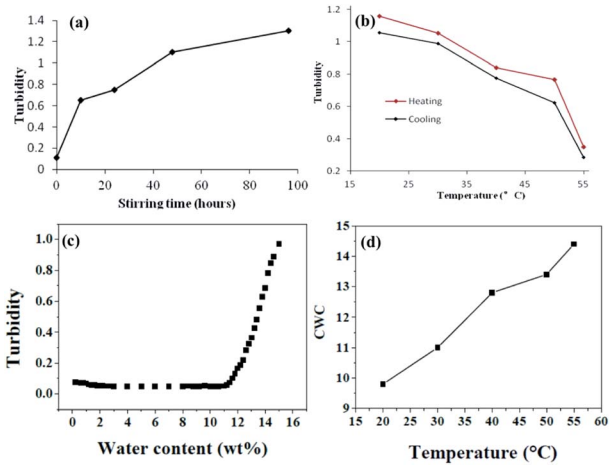

Fig. 7 (a) Change in turbidity with the stirring time; (b) change in turbidity with temperature during heating and cooling. All systems have an initial PS_{720}-*b*-$P2VP_{200}$-*b*-PEO_{363} concentration of 1.0 wt% and a 15 wt% water concentration in THF/water. (c) Turbidity change with the water content for 1.0 wt% PS_{720}-*b*-$P2VP_{200}$-*b*-PEO_{363} in THF; (d) critical water concentration (CWC) change with temperature for 1.0 wt% PS_{720}-*b*-$P2VP_{200}$-*b*-PEO_{363} in THF.

of two line segments (horizontal section and steeply increasing section).[33] The CWC change can more or less reflect the aggregation number of the polymeric chains quantitatively.[34] Obviously from Fig. 7d, CWC increases when increasing the temperature indicating that PS becomes less insoluble in the mixture of THF/water upon heating. These two factors might be the main reasons leading to the disassembly of the wormlike nanostructures upon increasing the temperature. Interestingly, when each of these samples at high temperatures is cooled back to room temperature in 1 hour by leaving the solutions away from the heat source, the segmented wormlike nanostructures are regenerated after stirring the solutions for four days at room temperature. This indicates that the morphological changes during heating and cooling are completely reversible.

We also follow the change in turbidity of the self-assembled process under stirring (1500 rpm) at different stages (Fig. 7a) and the disassembled process upon heating and quenched from high temperature (Fig. 7b). For a system with 1.0 wt% copolymer and 15 wt% water concentration in THF/water it is evident that the turbidity increases when increasing the stirring time (Fig. 7a). In contrast, the turbidity decreases when increasing the temperature. All the turbidity changes indicate the absence of the morphological transitions, which is corresponding with Fig. 6. Before using TEM to observe the morphologies after heating, samples were extracted from the solution mixture at different temperature, and then quenched by adding the extracted solutions to an excess of water. Turbidities before and after quenching were measured correspondingly. We can see from Fig. 7b that the turbidity changes during heating and quenching are identical which means quenching from high temperature to room temperature does not make a change to the morphology.

It is worth noting that neither intense stirring nor ultrasonic vibration could damage the structure of these wormlike nanostructures. To test this, the final solutions were placed into to ultrasonic bath (frequency 40 kHz, power 50 W) for about 30 min. The segmented wormlike nanostructures remained their original geometry without damage. These reflect the strong stability and the temperature responsive behavior of the structures, which makes the segmented wormlike nanostructures suitable vehicles to carry and release drugs when there is a temperature change.

Conclusions

In summary, this work demonstrates that PS-*b*-P2VP-*b*-PEO can self-assemble to form the segmented wormlike nanostructures through different processes. The segments of the structures can be not only perpendicular but also parallel to the main axis. And the length of the nanostructures depends on the stirring rate. To a certain extent, the stronger the shear field the longer the length of the nanostructures formed. However, only the triblock copolymer with proper compositions can self-assemble to form such giant segmented wormlike nanostructures. In addition, reversible morphological changes of these wormlike structures have been investigated upon changing the temperature. The segmented wormlike nanostructures can disassemble gradually, when increasing the temperature. With the strong stability of the nanostructures, we expect optimistically that such segmented aggregates from PS-*b*-P2VP-*b*-PEO would be potentially used in nanomedicine in the future.

Conflicts of interest

There are no conflicts to declare.

Acknowledgements

This work was funded by National Natural Science Foundation of China (22005141). We sincerely thank the Nanjing Tech University for the financial support (3983500183) and the Key Laboratory of Flexible Electronics (KLOFE) & Institute of Advanced Materials (IAM).

References

1 J. H. Kim, H. M. Jin, G. G. Yang, K. H. Han, T. Yun, J. Y. Shin, S. J. Jeong and O. K. Sang, *Adv. Funct. Mater.*, 2019, 1902049.
2 J. D. Hartgerink, E. Beniash and S. I. Stupp, *Science*, 2001, **294**, 1684.
3 Y. Geng, P. Dalhaimer, S. Cai, R. Tsai, M. Tewari, T. Minko and D. E. Discher, *Nat. Nanotechnol.*, 2007, **2**, 249.
4 Z. Li, E. Kesselman, Y. Talmon, M. A. Hillmyer and T. P. Lodge, *Science*, 2004, **306**, 98.
5 C. K. Wong, X. L. Qiang, A. H. E. Müller and A. H. Gröschel, *Prog. Polym. Sci.*, 2020, **102**, 101211.
6 J. H. Zhu, S. Y. Zhang, F. W. Zhang, K. L. Wooley and D. J. Pochan, *Adv. Funct. Mater.*, 2013, **23**, 1767.
7 Y. Q. Lu, J. P. Lin, L. Q. Wang, L. S. Zhang and C. H. Cai, *Chem. Rev.*, 2020, **120**, 4111.
8 D. J. Pochan, Z. Chen, H. Cui, K. Hales, K. Qi and K. L. Wooley, *Science*, 2004, **306**, 94.
9 Y. Matsushita, A. Takano, M. Vayer and C. Sinturel, *Adv. Mater. Interfaces*, 2020, 1902007.
10 F. He, T. Gädt, I. Manners and M. A. Winnik, *J. Am. Chem. Soc.*, 2011, **133**, 9095.
11 T. H. Epps, E. W. Cochran, C. M. Hardy, T. S. Bailey, R. S. Waletzko and F. S. Bates, *Macromolecules*, 2004, **37**, 7085.
12 M. W. Matsen and F. S. Bates, Origins of Complex Self-Assembly in Block Copolymers, *Macromolecules*, 1996, **29**, 7641–7644.
13 M. Huo, M. Zeng, D. Li, L. Liu, Y. Wei and J. Y. Yuan, *Macromolecules*, 2019, **52**, 1354.
14 J. Xin, D. Liu and C. L. Zhong, *J. Phys. Chem. B*, 2007, **111**, 13675.
15 T. P. Lodge, A. Rasdal, Z. Li and M. A. Hillmyer, *J. Am. Chem. Soc.*, 2005, **127**, 17608.
16 J. F. Gohy, N. Willet, S. Varshney, J. Zhang and R. Jérôme, *Angew. Chem., Int. Ed.*, 2001, **40**, 3214.
17 J. Babinot, E. Renard, B. D. Le, J. M. Guigner, S. Mura, J. Nicolas, P. Couvreur and V. Langlois, *Macromol. Rapid Commun.*, 2013, **34**, 362.
18 J. Huang, Y. K. Guo, S. Gu, G. Han, W. F. Duan, C. Q. Gao and W. Q. Zhang, *Polym. Chem.*, 2019, **10**, 3426.
19 H. Cui, Z. Chen, S. Zhong, K. Wooley and D. Pochan, *Science*, 2007, **317**, 647.
20 Z. Ma, H. Yu and W. Jiang, *J. Phys. Chem.*, 2009, **113**, 3333.
21 J. Zhu and W. Jiang, *Macromolecules*, 2005, **38**, 9315.
22 S. V. Aathimanikandan, E. N. Savariar and S. Thayumanavan, *J. Am. Chem. Soc.*, 2005, **127**, 14922.
23 K. Veronika and K. Eugenia, *ACS Appl. Polym. Mater.*, 2020, **2**, 26.
24 Q. R. Tian, C. H. Fei, H. Y. Yin and Y. J. Feng, *Prog. Polym. Sci.*, 2019, **89**, 108.
25 P. Bhargava, Y. Tu, J. Zheng, H. Xiong, R. P. Quirk and S. Z. D. Cheng, *J. Am. Chem. Soc.*, 2007, **129**, 1113.
26 Y. Xi, Y. Wang, J. Gao, Y. Xiao and J. Du, *ACS Nano*, 2019, **13**, 13645.
27 F. Wang, J. Gao, J. Xiao and J. Du, *Nano Lett.*, 2018, **18**, 5562.
28 H. Shen and A. Eisenberg, *Macromolecules*, 2000, **33**, 2561.
29 H. Yu and W. Jiang, *Macromolecules*, 2009, **42**, 3399.
30 S. Chiruvolu, S. Walker, J. Israelachvili, F. J. Schmitt, D. Leckband and J. A. Zasadzinski, *Science*, 1994, **264**, 1753.
31 C. Booth and D. Attwood, *Macromol. Rapid Commun.*, 2000, **21**, 501.
32 M. Almgren, J. Van Stam, C. Lindblad, P. Li, P. Stilbs and P. Bahadur, *J. Phys. Chem.*, 1991, **95**, 5677.
33 O. Terreau, C. Bartels and A. Eisenberg, *Langmuir*, 2004, **20**, 637.
34 H. Yu, J. Zhu and W. Jiang, *J. Polym. Sci., Part B: Polym. Phys.*, 2008, **46**, 1536.